Molecular Cell, Vol. 9, 563–573, March, 2002, Copyright ©2002 by Cell Press

The Genome-Wide Localization of Rsc9, a Component of the RSC Chromatin-Remodeling Complex, Changes in Response to Stress

Marc Damelin,[1,2] Itamar Simon,[3] Terence I. Moy,[1,2] Boris Wilson,[4] Suzanne Komili,[1,2] Paul Tempst,[5] Frederick P. Roth,[1] Richard A. Young,[3,6] Bradley R. Cairns,[4] and Pamela A. Silver[1,2,7]

[1]Department of Biological Chemistry and Molecular Pharmacology
Harvard Medical School
[2]The Dana-Farber Cancer Institute
1 Jimmy Fund Way
Boston, Massachusetts 02115
[3]Whitehead Institute for Biomedical Research
Nine Cambridge Center
Cambridge, Massachusetts 02142
[4]Howard Hughes Medical Institute and
Department of Oncological Science
Huntsman Cancer Institute
University of Utah
Salt Lake City, Utah 84112
[5]Molecular Biology Program
Memorial Sloan Kettering Cancer Center
New York, New York 10021
[6]Department of Biology
Massachusetts Institute of Technology
Cambridge, Massachusetts 02139

Summary

The cellular response to environmental changes includes widespread modifications in gene expression. Here we report the identification and characterization of Rsc9, a member of the RSC chromatin-remodeling complex in yeast. The genome-wide localization of Rsc9 indicated a relationship between genes targeted by Rsc9 and genes regulated by stress; treatment with hydrogen peroxide or rapamycin, which inhibits TOR signaling, resulted in genome-wide changes in Rsc9 occupancy. We further show that Rsc9 is involved in both repression and activation of mRNAs regulated by TOR as well as the synthesis of rRNA. Our results illustrate the response of a chromatin-remodeling factor to signaling cascades and suggest that changes in the activity of chromatin-remodeling factors are reflected in changes in their localization in the genome.

Introduction

Cells adapt to changes in the environment by activating defined programs of gene expression. The coordinated regulation of gene expression ensures appropriate responses to changes in nutrient availability, other forms of stress, and signals detected during development.

Two recent studies in the budding yeast *Saccharomyces cerevisiae* documented the transcriptional responses under many stress conditions and identified common sets of genes that are repressed or induced (Causton et al., 2001; Gasch et al., 2000). These studies also generalized the role of the transcriptional activators Msn2 and Msn4 in the stress response.

One of the signaling pathways known to regulate the activity of Msn2/4 is the TOR pathway (Beck and Hall, 1999). The TOR pathway controls cell growth in response to nutrient availability by regulating both transcription and translation (reviewed in Rohde et al., 2001; Schmelzle and Hall, 2000). Signaling is mediated by the TOR (Target of Rapamycin) kinases, which are specifically inhibited by the microbial product rapamycin (Schmelzle and Hall, 2000). Because of its antiproliferative activity, rapamycin is used as an immunosuppressant and offers potential for additional clinical applications (Rohde et al., 2001). Importantly, changes in gene expression resulting from rapamycin treatment closely parallel those of cells entering a state of starvation (Cardenas et al., 1999; Hardwick et al., 1999; Shamji et al., 2000).

Expression profiling in combination with genetic analysis has suggested that activators such as Msn2/4 do not account for all of the observed changes in the transcriptional response to stress. First, the mechanism underlying this response must account for extensive gene repression as well as activation (Causton et al., 2001; Gasch et al., 2000). Second, two lines of evidence indicate that the activation of many genes involves Msn2/4 only in some stress conditions (Gasch et al., 2000). On account of the broad changes in gene expression and the conditional involvement of activators, it is tempting to consider a role for general transcription factors in the stress response.

The regulation of gene expression is intimately connected to changes in chromatin structure (Kadonaga, 1998; Kingston and Narlikar, 1999). Protein complexes responsible for chromatin remodeling activity are conserved among eukaryotic cells (Kadonaga, 1998). RSC (Remodels the Structure of Chromatin) is an abundant 15 protein complex in *S. cerevisiae* that uses the energy of ATP hydrolysis to reposition nucleosomes. RSC was identified by homology to the SWI/SNF complex in yeast (Cairns et al., 1996), but only RSC is essential for viability and cell cycle progression (Angus-Hill et al., 2001; Cairns et al., 1996; Cao et al., 1997; Du et al., 1998; Laurent et al., 1992; Treich and Carlson, 1997; Tsuchiya et al., 1992). RSC has been isolated in distinct forms, containing either Rsc1 or Rsc2 and with or without Rsc3/Rsc30 (Cairns et al., 1996, 1999). Moreover, the RSC component Sfh1 is phosphorylated specifically during the G1 phase of the cell cycle (Cao et al., 1997). These results suggest that chromatin remodeling by RSC is regulated at compositional and posttranscriptional levels.

Genetic analysis of DNA binding domains present in many RSC components, an extensive analysis of RSC function at the *CHA1* promoter, and expression profiling in *rsc* mutants have implicated RSC in transcriptional regulation (Angus-Hill et al., 2001; Cairns et al., 1999; Moreira and Holmberg, 1999). However, the relationship

[7]Correspondence: pamela_silver@dfci.harvard.edu

between gene activity and RSC occupancy has not been established.

We have identified and characterized the Rsc9 protein, a component of the RSC complex. The genome-wide localization of Rsc9 revealed sites of occupancy throughout the genome and implied that Rsc9 targets many genes regulated by stress. We subsequently observed genome-wide changes in Rsc9 occupancy after treatment with rapamycin or hydrogen peroxide. Northern analysis confirmed a role for Rsc9 in the repression and activation of TOR-regulated genes. The results illustrate a role for this chromatin-remodeling factor in the transcriptional response to stress.

Results

RSC9 Encodes a Nuclear Protein with a DNA Binding Domain

RSC9 was identified by genetic and biochemical methods. The *rsc9-1* mutant was isolated in a screen for regulators of nuclear transport. In particular, we found that the essential transport receptor (karyopherin) Kap121 is trapped at the nuclear envelope in *rsc9-1* (Figure 1A; see also supplemental data at http://www.molecule.org/cgi/content/full/9/3/563/DCl). Cells harboring the *rsc9-1* mutation grow at 25°C, but 30°C incubation impairs growth, and temperatures above 34°C are cytotoxic. The *rsc9-1* mutation causes sensitivity to 15 mM caffeine and 2% formamide and a moderate sensitivity to 150 mM hydroxyurea—three common *rsc* phenotypes—but does not cause altered sensitivity to rapamycin (all at 25°C; data not shown). Homozygous *rsc9-1* diploids have a sporulation defect, as does another *rsc* mutant (Yukawa et al., 1999).

We observed a cell division defect in *rsc9-1*, as indicated by budding profiles of *rsc9-1* cells. After a 6 hr shift to 37°C, *rsc9-1* cells accumulate as large-budded (52.5% compared to 6.3% of wild-type) and multibudded (18.0% compared to 0.3% of wild-type). DNA staining showed that the buds of multibudded cells generally do not have nuclei, a common *rsc* phenotype. We performed FACS analysis on *rsc9-1* cells and observed a shift toward 2N and higher DNA content in *rsc9-1* cells at 37°C but not 25°C (Figure 1B).

The *rsc9-1* mutation maps to the previously uncharacterized open reading frame (ORF) *YML127w,* which we refer to as *RSC9.* Cells in which *RSC9* is deleted are not viable (data not shown), indicating that *RSC9* is essential for growth. The *RSC9* gene encodes a 581 residue, 63 kDa protein (Figure 1D). The *rsc9-1* allele has a Gln489→Stop mutation and may encode a truncated form of the protein.

Searches of genome databases with BLASTp (Altschul et al., 1990) revealed a homolog of Rsc9 in the fission yeast *Schizosaccharomyces pombe*, Spbc1703.02p. The sequences have 27% identity and 45% similarity ($E = 2 \times 10^{-16}$; Figure 1D). Both proteins contain an AT-rich interacting domain (ARID), a loosely defined DNA binding domain of ~100 residues present in *Drosophila* Dead Ringer and Osa, *S. cerevisiae* Swi1, human retinoblastoma binding proteins RBP1 and RBP2, and many others (Gregory et al., 1996; Herrscher et al., 1995) (Figures 1D and 1E). The Rsc9 and Dead Ringer ARIDs are highly conserved in the putative DNA recognition helix as determined by the structure of Dead Ringer (Iwahara and Clubb, 1999).

To localize the Rsc9 protein, we fused DNA encoding the green fluorescent protein (GFP) to the C terminus of *RSC9*. The *RSC9-GFP* fusion is functional since it restores growth in *rsc9*Δ cells and since a full-length fusion can be detected by immunoblot analysis (data not shown). Rsc9-GFP localizes exclusively to the nucleus during all phases of the cell cycle (Figure 1C).

Identification of Rsc9 as a Stable Component of the RSC Complex

To learn about the function of Rsc9, we performed a synthetic lethal screen with the *rsc9-1* allele, intending to identify mutations that, in combination with *rsc9-1*, render cells inviable at 25°C. We identified two extragenic recessive mutations that are lethal in combination with *rsc9-1* (PSY2351, 2352; see Table 1). The mutations are in genes encoding two RSC members, Sth1 and Rsc8. These results suggested that Rsc9 might be a component of RSC. The *sth1-101* allele has a T→C mutation in the coding strand, changing Leu122 to Ser in the protein sequence. The *rsc8-1* allele has a G→A mutation, changing the conserved Glu348 to Lys.

Biochemical evidence for Rsc9 as a member of RSC was acquired through purification, mass spectrometry, and peptide sequencing. To identify Rsc9, the diffuse 66 kDa protein band was excised from an SDS-PAGE gel of purified RSC (Figure 2A), and peptides were analyzed by MALDI-TOF mass spectrometry. Identification of *RSC9* as ORF *YML127w* was established by mass fingerprinting of 11 peptides and Edman sequencing of the peptides CCFEPVQEAEFTZIxL and SIHTSL ANFNVFQSLPK, which correspond to residues 401–418 and 57–73, respectively.

To further characterize the association of Rsc9 with the RSC complex, we partially purified Rsc9 using an Rsc9 derivative tagged with protein A. Two experiments established that Rsc9 is tightly associated with RSC. First, Rsc9 and other RSC components showed identical elution profiles from the cation exchange matrix SP (data not shown). Second, Rsc9-protein A and RSC components bind to an IgG sepharose column and are retained after stringent washing (Figure 2B). These results establish Rsc9 as a stable component of RSC complex.

Genome-Wide Localization of Rsc9

The RSC complex is very abundant—estimated at 1000–2000 copies per cell—and has the potential to act at a proportional number of loci. To identify RSC targets, we performed the genome-wide localization of Rsc9. This experiment explores protein-DNA interactions on the genomic scale by combining chromatin immunoprecipitation with microarray analysis (Iyer et al., 2001; Ren et al., 2000). In general, the genome-wide localization of a wild-type protein sidesteps a potential shortcoming of expression profiling in deletion and temperature-sensitive mutants, which may have limited variations in steady-state gene expression.

To perform the experiment, the genomic copy of *RSC9* was replaced by a functional *RSC9-myc* fusion. The *RSC9-myc* cells were later found to be *rho*$^{-}$, but this

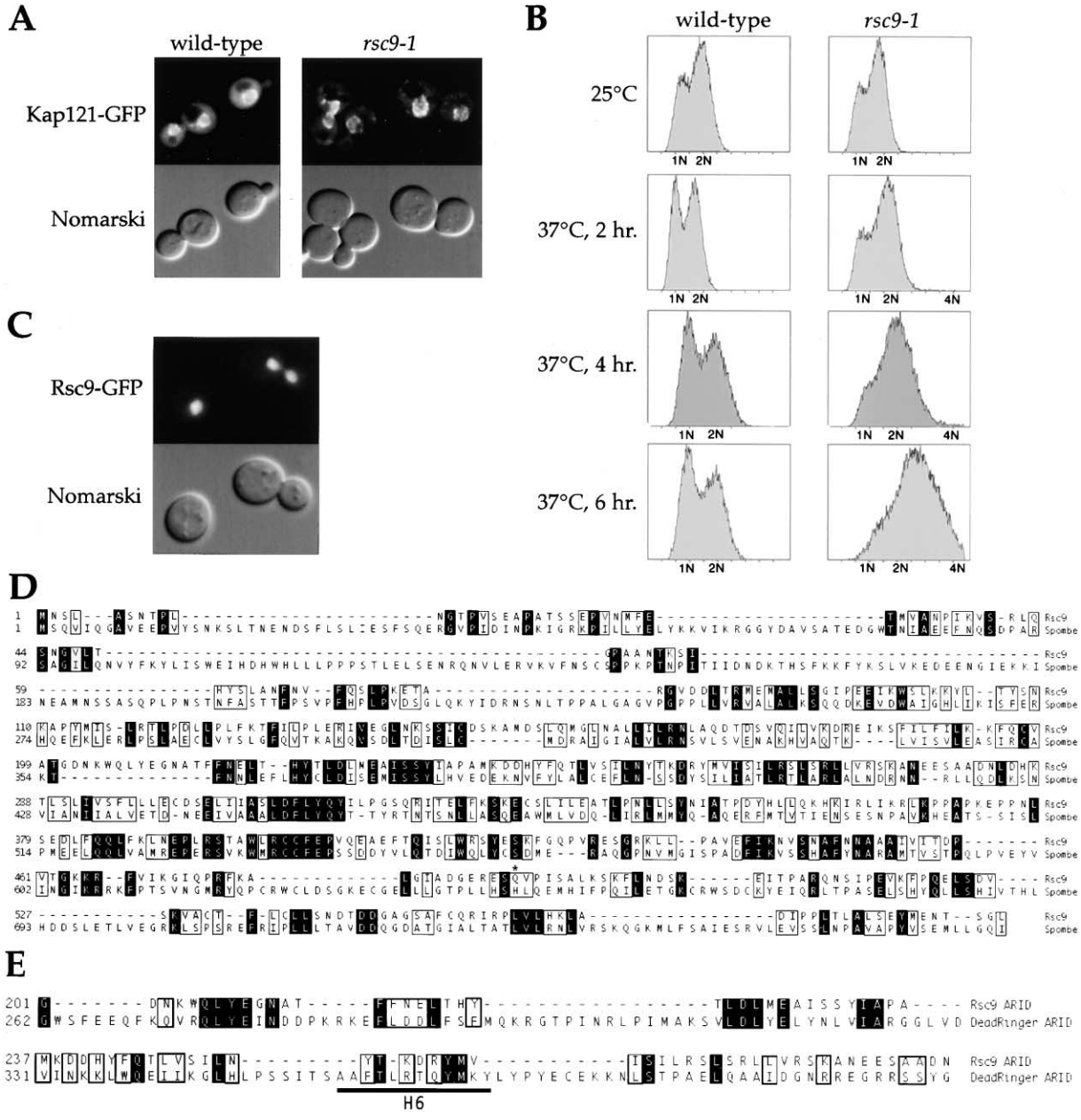

Figure 1. Characterization of the *rsc9-1* Mutation and the Rsc9 Protein

(A) Wild-type (left) and *rsc9-1* (right) cells expressing Kap121-GFP were grown to log phase at 25°C, shifted to 37°C for 100 min, and examined by fluorescence microscopy with a GFP filter set (top) and Nomarski optics (bottom). Representative cells from different fields are shown.

(B) FACS analysis of *rsc9-1*. Wild-type and *rsc9-1* cells were grown in YPD at 25°C to log phase (top panels) and shifted to 37°C for 2, 4, or 6 hr.

(C) Cells expressing Rsc9-GFP were examined by microscopy.

(D) Sequence alignment of the *S. cerevisiae* Rsc9 protein and its closest known homolog, *S. pombe* Spbc1703.02p, was performed with the Clustal algorithm in MegAlign (DNASTAR). The ARID of Rsc9 comprises residues 200–283. Identical residues are shaded and similar residues are boxed. Gln489, which is mutated to a stop codon in *rsc9-1,* is marked with an asterisk.

(E) Alignment of the AT-rich interacting domains (ARIDs) of Rsc9 and *Drosophila* Dead Ringer was performed as in (D). The putative DNA-recognition helix of the Dead Ringer ARID is indicated by H6.

characteristic does not impact our results (see Experimental Procedures). The cells were grown in rich media containing glucose to logarithmic phase and treated with formaldehyde to crosslink proteins and DNA. Chromatin was isolated and sheared, and the DNA fragments associated with Rsc9 were enriched by immunoprecipitation of Rsc9-myc. These fragments were amplified and labeled with the Cy5 fluorophore by ligation-mediated PCR. DNA fragments from the whole-cell extract were amplified and labeled with the Cy3 fluorophore and served as the standard. The samples were competitively hybridized to a microarray containing all of the intergenic

Table 1. Yeast Strains Used in This Study

Strain	Genotype	Source
PSY2345	*PSE1-GFP::TRP1 trp1Δ63 ura3-52 leu2Δ1 mata*	Seedorf et al., 1999
PSY2346	*PSE1-GFP::URA3 ura3-52 trp1Δ63 leu2Δ matα*	This study
PSY2347	*rsc9-1 PSE1-GFP::TRP1 trp1Δ63 ura3-52 leu2Δ1 mata*	This study
PSY2348	*rsc9-1 ura3-52 trp1Δ63 his3Δ200 leu2Δ1 mata*	This study
PSY2349	*rsc9-1 ade3 ade2 ura3-52 trp1Δ63 his3Δ200 leu2Δ1 mata <RSC9 URA3 ADE3>*	This study
PSY2350	*rsc9-1 ade3 ade2 ura3-52 his3Δ200 leu2Δ1 matα*	This study
PSY2351	*rsc9-1 sth1-101 ade3 ade2 ura3-52 trp1Δ63 leu2Δ1 mata <RSC9 URA3 ADE3>*	This study
PSY2352	*rsc9-1 rsc8-1 ade3 ade2 ura3-52 trp1Δ63 leu2Δ1 matα <RSC9 URA3 ADE3>*	This study
PSY2353	*sth1-101[L122S] ura3-52 trp1Δ63 leu2Δ1 ade3 ade2 matα*	This study
PSY2354	*rsc8-1[E348K] ura3-52 trp1Δ63 leu2Δ1 ade3 ade2 matα*	This study
PSY2355	*RSC9-prA-6xHis::TRP1 trp1Δ63 ura3-52 leu2Δ1 mata*	This study
Z1256	*ade2-1 leu2-3,112 his3-11,15 trp1-1 ura3-1 can1-100 mata [W303]*	Cosma et al., 1999
PSY2439	*RSC9-18xMYC::TRP1 ade2-1 leu2-3,112 his3-11,15 trp1-1 ura3-1 can1-100 mata rho−*	This study
PSY2359	*nup133-1 ura3-52 trp1Δ63 leu2Δ1 matα*	This study
PSY2360	*nup133-2 ura3-52 trp1Δ63 leu2Δ1 his3Δ200 matα*	This study
PSY2361	*tps2-101 ura3-52 trp1Δ63 leu2Δ1 his3Δ200 mata*	This study
PSY2362	*tps2-102 ura3-52 trp1Δ63 leu2Δ1 his3Δ200 mata*	This study

sequences in the yeast genome (Ren et al., 2000). After background subtraction, the ratio of immunoprecipitation-enriched signal to whole-cell extract signal at each spot on the microarray was calculated, the spots were sorted by ratio, and a percentile was assigned to each spot (e.g., the 90th percentile denotes that 90% of all spots on that microarray have lower ratios). The experiment was performed in triplicate, and the median of the three percentile values for each spot was used to generate a list of intergenic sequences ordered by degree of enrichment. This list was translated to a ranked list of ORFs. The complete data sets are available (see supplemental data at http://www.molecule.org/cgi/content/full/9/3/563/DCI).

Our approach to the data analysis was shaped by two issues intrinsic to a general factor: the need to determine a threshold of Rsc9 occupancy and the importance of considering broad relationships among genes targeted by a general transcription factor. To this end, we used a computer program that searches for enrichments among Rsc9 targets of genes in functional categories defined by a single attribute, such as a biochemical activity or subcellular localization. The program combines the occupancy data with information in the YPD database (Costanzo et al., 2001) to identify the enrichments and calculate a statistic describing the significance of each enrichment.

There are two inputs to the program: the ranked list

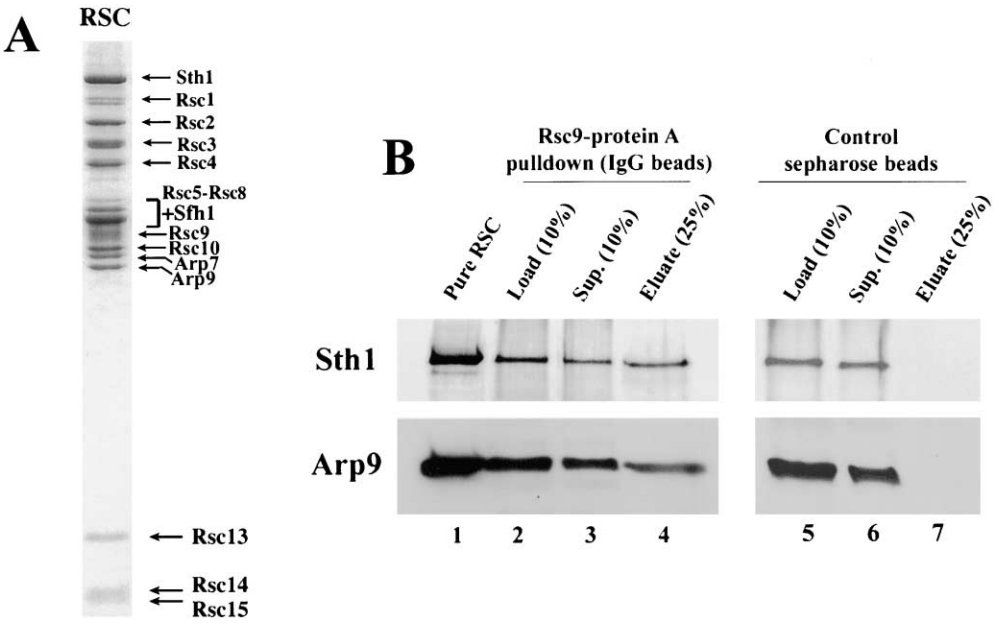

Figure 2. Biochemical Characterization of Rsc9

(A) Pure RSC utilized for mass spectrometric analysis and peptide sequencing. Sample shown was stained with Coomassie dye (Cairns et al., 1996).

(B) Rsc9 is tightly associated with RSC. RSC was partially purified from a strain expressing Rsc9-protein A (see Experimental Procedures). The following samples were subjected to SDS-PAGE and immunoblot analysis: pure RSC (1 μg; lane 1), load (100 μg, 10% of input; lanes 2 and 5), supernatant (100 μg, 10% of input; lanes 3 and 6), and SDS eluate (25%; lanes 4 and 7).

of ORFs from the genome-wide localization, and a list of functional categories and the genes in each category as annotated in YPD. For each category, the distribution of the genes within the ranked list is assessed, and the significance associated with each identified enrichment is calculated with Fisher's exact test. By repeating this calculation at different cutoffs within the ranked list, a cutoff corresponding to the maximum statistical enrichment for that category is determined. Multiple hypothesis corrections are based on simulations with randomly generated lists (see Experimental Procedures). Each reported p value represents the probability that the observed enrichment could happen by chance.

We identified two categories with significant enrichments among Rsc9-occupied sites. The category of ribosome-associated factors, consisting mostly of the genes encoding the cytoplasmic and mitochondrial ribosomal proteins, is highly enriched ($p = 0.005$; Figure 3A). The p value is below the standard threshold of 0.05, indicating the significance of the enrichment. The category of genes encoding proteins involved in the stress response, including many genes activated by Msn2 and Msn4, is also enriched ($p = 0.045$; Figure 3A). The expression of genes in both of these categories is affected by general stress as well as TOR signaling. Both enrichments are specific to Rsc9, as they are not observed in the data sets for the Ste12 and Gal4 transcription factors (Ren et al., 2000).

The cutoff points in the ranked list corresponding to the maximum statistical enrichments in both categories are very close, at the 71st and 72nd median percentile (Figure 3A). The peak cutoff point for a third category enriched in a different Rsc9 localization experiment is also in this region (see below). The consistency among independent categories suggests that a threshold for Rsc9 occupancy can be assigned at that point in the ranked list, corresponding to about 1700 intergenic regions.

Our analysis also indicated that most genes in the nitrogen discrimination pathway (NDP) are targeted by Rsc9. Sixteen of the 24 NDP genes are above the 71st median percentile, and 21 of 24 are above the 50th; however, because this category contains only 24 genes, the enrichment is not statistically significant. The NDP genes are induced through inhibition of the TOR signaling pathway—for example, in environments with poor-quality nitrogen sources (Cardenas et al., 1999; Hardwick et al., 1999; Shamji et al., 2000).

We also identified a correlation between Rsc9-occupied sites and the cell cycle. Many cell cycle genes are targeted by Rsc9, most notably those of the histones. Several cyclins, including *CLB5,* are also targeted. These results are consistent with the cell division defects of *rsc9-1*. Interestingly, a recent study has implicated Clb5 in a role in the TOR pathway (Chan et al., 2000).

The results from our genome-wide localization of Rsc9 are consistent with several data on the RSC complex. For example, the levels of many stress- and TOR-regulated genes are affected in *rsc3-2* and *rsc30Δ,* including over 100 ribosomal-protein (RP) genes as well as *PUT1, PRB1, SSA4, HSP12, HSP26, HSP30, TPI1, CUP5, COX5A, SOD1, TTR1, TRX2, TSA1, OYE3, SDH3, TDH3, HOR7, HXT3, HXT4, HXT6, TEF4,* and *TIF11* (Angus-Hill et al., 2001). This correlation extends to genes involved in cell wall maintenance, many of which are among the Rsc9-occupied sites and whose expression levels are affected in *rsc3* and *rsc30* (Angus-Hill et al., 2001). Furthermore, the data from our Rsc9 localization are substantiated by work on the *CHA1* gene. *CHA1* is constitutively repressed under normal growth conditions, and Sth1 and Rsc8 are required for the repression (Moreira and Holmberg, 1999). *CHA1* is in the 96th median percentile of Rsc9 occupancy, consistent with the role of RSC in its constitutive repression. Taken together, these correlations suggest that the genome-wide localization of Rsc9 can be generalized to other RSC components.

Two Stress Treatments Cause Genome-Wide Changes in Rsc9 Localization

Expression of genes in both the ribosome-associated and cell stress categories are affected by many types of stress (Causton et al., 2001; Gasch et al., 2000); thus, we hypothesized that RSC might be involved in the stress response. The occupancy of many NDP genes, which are induced by only a subset of stress conditions, raised the question of whether RSC responds to specific or general stress.

We reasoned that if RSC were involved in the stress response, then the localization of RSC would change accordingly. Thus, we repeated the genome-wide localization of Rsc9 in cells treated with either hydrogen peroxide, which elicits a transcriptional response similar to many other stresses (Causton et al., 2001; Gasch et al., 2000), or rapamycin, which induces the expression of additional sets of genes such as the NDP. Treatments lasted 30 min, at which point significant changes in gene expression were observed. In both cases we found that the occupancy patterns of Rsc9 are different in treated versus untreated cells (Figure 3). In contrast, an untreated sample processed in parallel yielded results similar to the original untreated samples (data not shown).

Our analysis program revealed that the functional categories enriched in untreated cells are no longer enriched in rapamycin- or hydrogen peroxide-treated cells (Figure 3A). These include ribosome-associated factors, cell stress factors, and the NDP genes. However, occupancy at the histone genes remains unchanged; since their expression is unaffected by either treatment, these results demonstrate the specificity of the observed changes in Rsc9 occupancy.

Strikingly, rapamycin treatment causes an enrichment among Rsc9 targets of genes encoding mitochondria-localized proteins ($p = 0.007$; Figure 3A), although no enrichment is detected in untreated cells. This category includes genes for oxidative phosphorylation, ATP synthesis, ubiquinone synthesis, and the TCA cycle, all of which are induced following rapamycin treatment (Hardwick et al., 1999). The cutoff for maximum statistical enrichment is the 74th median percentile, similar to the cutoffs described above.

We compared the rapamycin- and hydrogen peroxide-induced changes in Rsc9 occupancy at the genes in the above categories with the changes in their expression (Figure 3B). We used the 71st median percentile as the cutoff for defining Rsc9 occupancy. The expression data were taken from studies using the same experimental conditions (Gasch et al., 2000; Shamji et al., 2000).

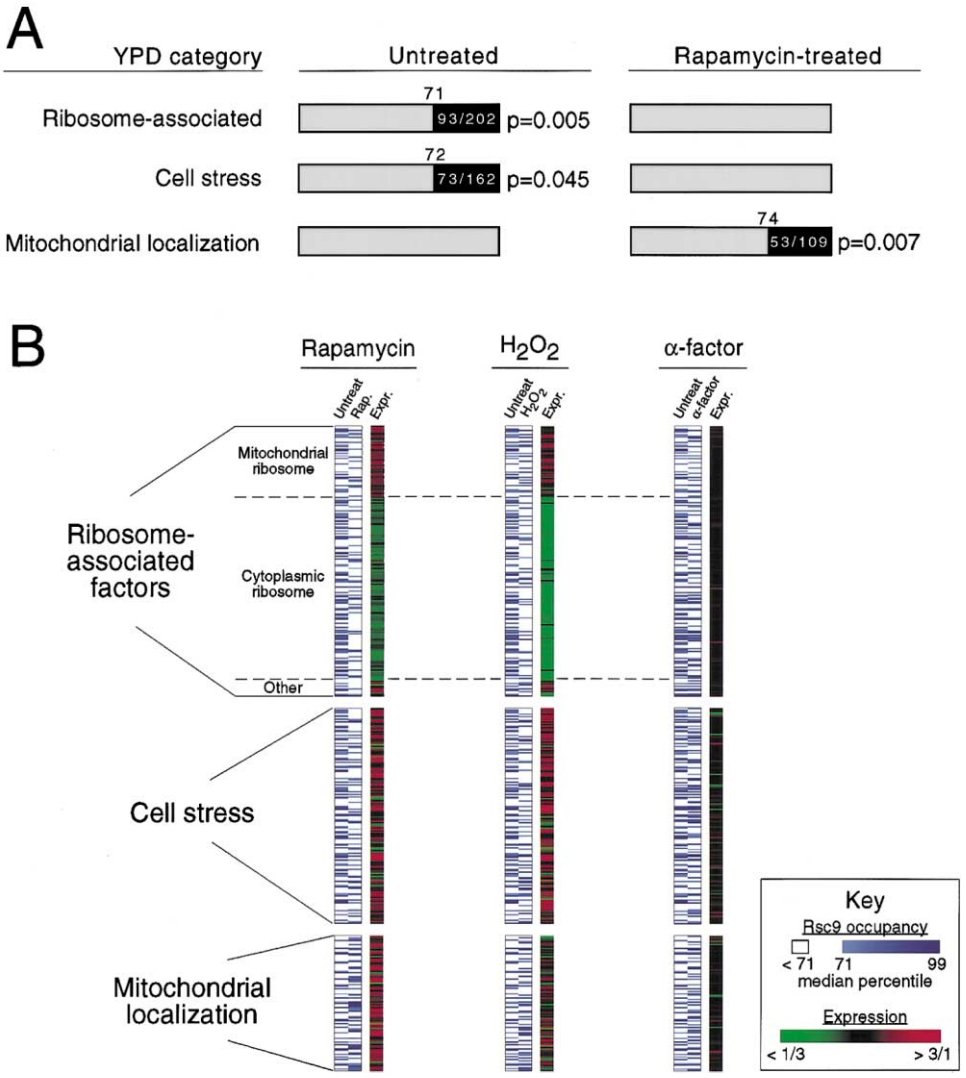

Figure 3. Genome-Wide Localization of Rsc9 and the Effect of Various Treatments

(A) Schematic representation of the enrichment of genes in YPD categories among Rsc9-occupied sites. The enrichments were identified and statistically evaluated by the analysis program described in the text. The distribution of genes in a given category before and after rapamycin treatment is shown as follows. Each bar represents the entire ranked list of ORFs, from 99th median percentile (right) to zero (left). The black portion represents the enrichment of genes in a category, with the fraction of genes present in that portion of the list indicated in white text. The number above the black portion indicates the median percentile cutoff corresponding to the maximum statistical enrichment. The gray portions of the bars represent the lack of enrichment (but not the absence) of genes in that category.

(B) Comparison of changes in Rsc9 occupancy to changes in gene expression for three treatments. The occupancy before (Untreat) and after (Rap., H_2O_2, or α factor) treatment is displayed using a blue-white color scheme, and the expression ratios (treated to untreated) of genes are displayed using a red-green color scheme; both representations were generated with TreeView (Eisen et al., 1998). Expression data were taken from Shamji et al., 2000 (rapamycin), Gasch et al., 2000 (hydrogen peroxide), and Roberts et al., 2000 (α factor) for the same conditions used in the genome-wide localization. Data are shown only for the functional categories that show enrichments with respect to Rsc9 occupancy.

We found that the relationship between change in Rsc9 occupancy and change in expression depended on the functional category, suggesting distinct roles for Rsc9 at the respective promoters. The stress-induced decrease in occupancy at the ribosome-associated factors is concentrated in the cytoplasmic RP genes, which are repressed under stress. In contrast, while occupancy of the cell-stress genes also decreases, many of these genes are activated under stress. The NDP genes, which are activated by rapamycin, also show decreased occupancy after rapamycin treatment. Finally, occupancy of genes in the mitochondrial localization category increases with rapamycin when most of these genes are activated. In response to hydrogen peroxide, both the occupancy and expression of the genes in this category change in the same direction as with rapamycin but not to the same extent.

The similar changes of Rsc9 localization after both treatments suggested a general stress response but prompted us to ask whether the changes would occur from an unrelated treatment. To this end, we performed the genome-wide localization of Rsc9 after treatment with the mating pheromone α factor, which generally does not affect the expression levels of RP and cell-

	ORF	Rsc9 occupancy (median percentile) Untr.	Rap.	αF
Induced	*YMR315W*	37	53	76
	YFR053C (HXK1)	83	80	86
	YGL053W (PRM8)	77	52	36
	YDL022W (GPD1)	83	85	89
	YJL163C	35	91	59
	YDL023C	36	52	52
	YHR097C	76	75	71
	YJL218W	80	49	47
	YIL082W	66	55	61
	YOL150C	5	25	37
	YOR347C (PYK2)	69	66	49
	YLR327C	92	87	86
Repressed	*YML108W*	12	42	60
	YLR397C (AFG2)	42	96	80
	YKL029C (MAE1)	73	43	83

Figure 4. Rsc9 Occupancy at Genes Coregulated by Rapamycin and α Factor

ORFs induced or repressed at least 2-fold in response to both rapamycin treatment and α factor treatment were identified from published data sets (Roberts et al., 2000; Shamji et al., 2000) for the same conditions used in the genome-wide localization. Rsc9 occupancy at these genes is shown in terms of the median percentile value for untreated (Untr.), rapamycin-treated (Rap.), or α factor-treated (αF) cells. Individual ORFs were examined for relative changes in Rsc9 occupancy under each treatment; relative change was defined as at least a 2-fold increase in distance from either end of the ranked list. Changes with rapamycin or α factor (compared to untreated) are highlighted.

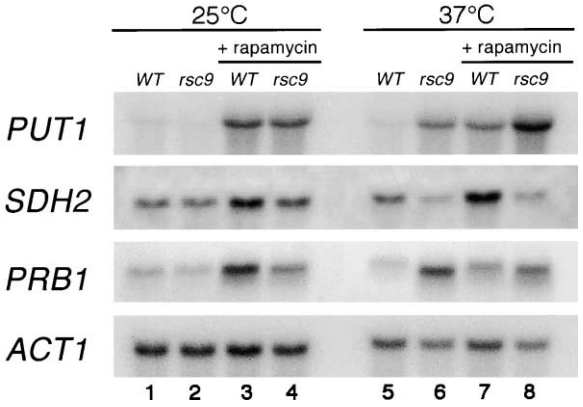

Figure 5. RSC Affects the Expression of Genes in the TOR Pathway

Wild-type cells (lanes 1, 3, 5, and 7) and *rsc9-1* cells (lanes 2, 4, 6, and 8) were grown at 25°C (lanes 1–4) and shifted to 37°C for 3 hr (lanes 5–8). Samples were treated with rapamycin (200 nM; lanes 3, 4, 7, and 8) or mock treated with DMSO (lanes 1, 3, 5, and 6). Northern analysis was perfomed on *PUT1*, *SDH2, PRB1*, or *ACT1.*

stress genes (Figure 3B). Following α factor treatment, Rsc9 occupancy of the RP genes is still enriched, though not to the same extent as in untreated cells. Furthermore, occupancy of the cell-stress and NDP genes is comparable to untreated cells. There was some change but no significant enrichment in the mitochondrial localization category. In sum, the stress-induced changes in category-based enrichments are not observed with α factor treatment.

In an alternative approach to analyzing the occupancy data, we examined Rsc9 occupancy patterns at the genes affected by both rapamycin and α factor. In total, 12 ORFs are induced at least 2-fold and three ORFs are repressed at least 2-fold in response to both treatments (compiling data from Roberts et al., 2000 and Shamji et al., 2000). The median percentile values from the Rsc9 occupancy data in untreated, rapamycin-treated, and α factor-treated cells are shown for this set of genes in Figure 4. Rapamycin-induced changes in Rsc9 occupancy are observed for 47% (7/15) of these genes, a proportion comparable to that observed for the functional categories in Figure 3. Since the expression of these particular genes is similarly affected by both rapamycin and α factor, Rsc9 occupancy at these genes should also be similarly affected if the occupancy data are meaningfully related to transcriptional regulation. Indeed, 71% (5/7) of the ORFs showing occupancy changes after rapamycin treatment also show changes after α factor treatment, implying functional significance in the Rsc9 occupancy data. This analysis is both complementary to and consistent with the analysis by functional category.

The Expression of Several TOR-Regulated Genes Is Affected by the *rsc9-1* Mutation

The comparison between changes in gene expression and Rsc9 occupancy implied that Rsc9 is involved both in the repression and activation of stress-regulated genes. To test this hypothesis, we performed Northern analysis in the *rsc9-1* mutant on genes with different expression-occupancy relationships. We focused on genes regulated by the TOR pathway, since some genes targeted by Rsc9, including the NDP genes, are induced by rapamycin but not hydrogen peroxide. Indeed, we found roles for Rsc9 in both the repression and activation of TOR-regulated genes, consistent with predictions from the genome-wide localization.

To determine whether Rsc9 is involved in the repression of NDP genes, we examined the *PUT1* and *PRB1* genes. Expression levels were compared in wild-type and *rsc9-1* cells with or without rapamycin treatment. We found that *PUT1* expression was 10-fold higher in untreated *rsc9-1* compared to wild-type at 37°C (Figure 5, lanes 5 and 6). Following rapamycin treatment, levels of *PUT1* were 4-fold higher in *rsc9-1* at 37°C (Figure 5, lanes 7 and 8). Similarly, *PRB1* expression was 9-fold higher in *rsc9-1* without treatment and 2.5-fold higher with rapamycin treatment at 37°C (Figure 5, lanes 5 and 6, 7 and 8). Thus, the expression levels of *PUT1* and *PRB1* both in noninducing and inducing conditions are higher in *rsc9-1*. Expression profiling revealed that *PUT1* and *PRB1* levels are also increased in another *rsc* mutant, *rsc3-2* (Angus-Hill et al., 2001). These results suggest that RSC functions in the constitutive repression of *PUT1* and *PRB1*.

To determine whether Rsc9 is involved in the activation of genes in the mitochondrial localization category, we examined the expression of *SDH2,* a gene in the TCA cycle. We found that the induction of *SDH2* by rapamycin is not observed in *rsc9-1*. Expression of *SDH2* increases nearly 2-fold in wild-type cells after rapamycin treatment, but is not induced at all in *rsc9-1* (Figure 5, lanes 7 and 8). The effect of the *rsc9-1* mutation on *SDH2* expression contrasts sharply with its effect on *PUT1* and *PRB1* expression, demonstrating that Rsc9 is involved in both the repression and activation of TOR-regulated genes.

The opposing effects of *rsc9-1* on the expression of *PUT1* and *PRB1* versus *SDH2* are matched by different

rapamycin-induced changes in Rsc9 occupancy at their promoters. *PUT1* is in the 96th median percentile in untreated cells and the 59th after treatment; similarly, *PRB1* decreases from 97th to 81st. In contrast, *SDH2* increases from the 42nd median percentile in untreated cells to the 95th after treatment. The Northern analysis is thus consistent with the genome-wide localization data and, together with the expression profiles of *rsc3* and *rsc30* mutants (see above), shows a role for RSC in rapamycin-induced repression and activation. The data also provide three examples in which a change in Rsc9 function at a given locus is reflected in a change in Rsc9 occupancy at that locus.

Defect of *rsc* Mutants in Ribosome Biogenesis

The stress-dependent enrichment among Rsc9-occupied sites of RP genes (Figure 3) and the relationship between stress and ribosome biogenesis (Powers and Walter, 1999) prompted us to explore whether RSC functions in ribosome biogenesis. A fusion of GFP to the large ribosomal subunit protein Rpl11b was monitored during growth at different temperatures as described (Stage-Zimmermann et al., 2000). Cells were grown at 25°C, shifted to 37°C, and then shifted back to 25°C. The upregulation of ribosome synthesis upon the shift back to 25°C enables defects in assembly and export to be visualized by nuclear accumulation of the reporter protein (Figure 6A).

Rpl11b-GFP mislocalizes to the nucleus in two RSC mutants, *rsc9-1* and *sth1-101* (Figure 6B). These results indicate that the biogenesis of the large ribosomal subunit is affected in these mutants. No defect in the ratio of free 60S:40S subunits or in rRNA processing was observed in *rsc9-1* or *sth1-101* (data not shown).

Defect of the *rsc9-1* Mutant in rRNA Synthesis

We also explored the role of RSC in ribosome biogenesis by investigating rRNA synthesis in *rsc9-1*. Wild-type and *rsc9-1* cells were labeled for 3 min with ^{3}H-methionine, which is incorporated primarily into rRNA (and to a small degree into mRNA and tRNA). Total RNA was isolated, and the amount of newly synthesized rRNA was calculated by taking the ratio of radioactive counts (rRNA) to OD_{260} (total RNA). This approach allows an approximate measurement of rRNA synthesis in vivo; however, mutations affecting transcription versus methylation cannot be distinguished.

Shifting wild-type cells to 37°C causes a temporary decrease in ribosome biogenesis (Warner, 1989), but the cells recover and increase rRNA synthesis after a 3 hr shift (Figure 6C). In contrast, rRNA synthesis in *rsc9-1* is reduced at this time point (Figure 6C). Cells harboring the unrelated temperature-sensitive mutation *npl3-1* do not show this defect. These results further indicate that RSC plays a role in ribosome biogenesis, a principal target of the stress response.

Discussion

We have identified Rsc9 as a component of the abundant chromatin remodeling complex RSC. Our analysis has demonstrated that Rsc9 occupies and regulates—both positively and negatively—targets of the stress response, including genes regulated by the TOR pathway. The changes in genome-wide localization of Rsc9 under stress conditions suggest that signal transduction pathways could influence RSC targeting in the genome.

Rsc9, an RSC Component with a DNA Binding Domain

We have presented several lines of evidence indicating that Rsc9 is a functional member of RSC. Rsc9 was identified as a component of the purified RSC complex. The *rsc9-1* mutation has genetic interactions with other *rsc* mutations and shares several phenotypes with them. Rsc9, like the other characterized RSC proteins, localizes to the nucleus and is encoded by an essential gene.

Rsc9 contains an AT-rich interacting domain, a DNA binding domain. Different DNA binding domains are present in other RSC members, including the AT hooks in Rsc1 and Rsc2 (Cairns et al., 1999) and the zinc clusters in Rsc3 and Rsc30 (Cairns et al., 1998). The presence of various DNA binding domains in RSC may allow for a high degree of target discrimination, and how each of these motifs contributes to the recognition of particular DNA sequences will be important for understanding RSC function.

An Integrative Analysis of the Rsc9 Genome-Wide Localization

The relationship between RSC and the stress response became evident from an analysis of Rsc9 genome-wide localization that considered categories of functionally related genes. This approach provides a powerful means for interpreting genome-based data because of its ability to integrate new data with the wealth of available information. Moreover, with this approach we could address two issues inherent in the data analysis for an abundant general factor. First, the median percentile values corresponding to the maximum statistical enrichments provided a means of identifying a threshold for Rsc9 occupancy in the ranked list. (The bimodal distribution observed for some activators is not expected for a general factor that occupies many more sites.) Second, the category-based analysis provided a broad perspective from which to identify trends in the data. The approach also reduces the consequences of false positives and false negatives that are inevitable in genomics data by generating statistics to describe each enrichment and by not focusing on individual genes.

Our studies have focused on Rsc9, but independent observations suggest that the connection to the stress response also involves other RSC components. First, expression profiling of *rsc3-2* and *rsc30*Δ showed that the levels of many stress- and TOR-regulated genes are affected (see Results). Second, the occupancy of Rsc9 at *CHA1* is consistent with previous results for Rsc8 and Sth1. Third, the defect in ribosome biogenesis is observed for both *rsc9-1* and *sth1-101*. However, the results technically apply only to Rsc9, and the stress response might involve only a subset of RSC complexes.

Rsc9 Can Assist the Repression or Activation of Genes Regulated by TOR Signaling

Our data suggest that Rsc9 is important for the repression of TOR-regulated genes. For example, the NDP genes are occupied by Rsc9 in untreated cells, when they are repressed, and are not occupied by Rsc9 in rapamycin-treated cells, when they are activated. Two

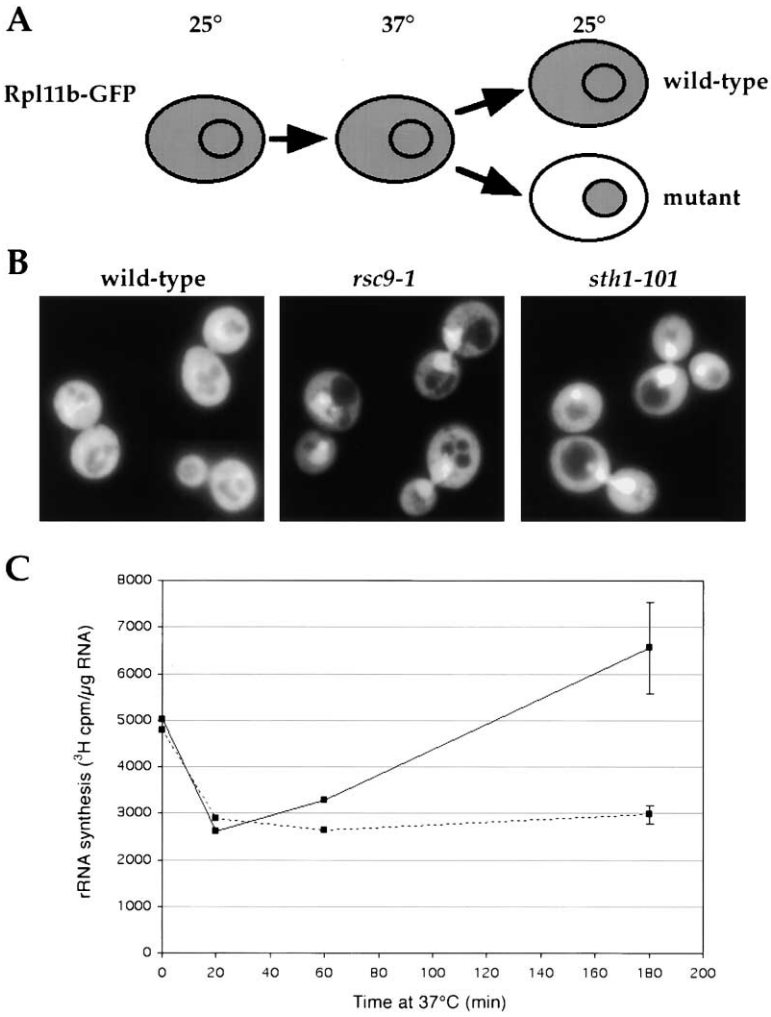

Figure 6. Ribosome Biogenesis and rRNA Synthesis Defects in *rsc* Mutants

(A) Schematic diagram of an assay for the export of the large ribosomal subunit.

(B) Wild-type, *rsc9-1*, and *sth1-101* cells expressing Rpl11b-GFP were grown at 25°C, shifted to 37°C for 2 hr, shifted back to 25°C for 20 min, and examined by microscopy.

(C) Production of rRNA in rsc mutants. Wild-type (solid line) and *rsc9-1* cells (dotted line) cells were grown at 25°C to a density of 10^7 cells/ml in synthetic media lacking methionine, shifted to 37°C for 20, 60, or 180 min, and labeled with [methyl-^{3}H]methionine for 3 min. Total RNA was isolated from each sample, and the ratio of radioactive counts (methylated rRNA) to OD_{260} (total RNA) was calculated.

NDP genes, *PUT1* and *PRB1,* are aberrantly expressed in the *rsc9-1* mutant, thus independently demonstrating that Rsc9 is involved in their constitutive repression. A role for RSC in gene repression has been suggested (Angus-Hill et al., 2001; Moreira and Holmberg, 1999), but these studies did not address RSC occupancy of these genes. In the current study, the combination of stress-dependent occupancy and expression demonstrates a direct involvement for RSC.

Similarly, our results suggest a role for Rsc9 in the activation of TOR-regulated genes. Rsc9 occupies promoters of genes encoding certain mitochondrial proteins only after rapamycin treatment, when those genes are activated. *SDH2* expression is increased by rapamycin treatment in wild-type cells, whereas in the *rsc9-1* mutant no change is observed, implying that Rsc9 is required for the induction of *SDH2*. Previous studies have suggested a role for RSC in gene activation (Angus-Hill et al., 2001; Yukawa et al., 1999), but again these studies did not address RSC occupancy and thus did not observe a direct role for RSC.

Taken together, our results suggest that the stress-induced changes in Rsc9 genome-wide localization are functionally significant. Two assays for ribosome biogenesis provided further evidence for a role for RSC in the stress response.

Signaling Pathways and Chromatin Remodeling

These studies illustrate the response of a chromatin-remodeling factor to cellular signaling. The shifts in Rsc9 localization suggest a novel phenomenon of genome conditioning during widespread transcriptional changes. Our results raise new and interesting questions for transcriptional regulation. First, how does signaling affect RSC targeting—are interactions between RSC and chromatin, activators, and repressors affected by modifications (such as phosphorylation) directed toward RSC or the others? Second, how can a remodeler promote activation at one locus and repression at another—does each locus have certain properties that determine the effect of RSC occupancy (such as nucleosome positioning), or is RSC function modified in some way? Stress responses generate a variety of intracellular signals affecting transcriptional regulation; identifying how each of these signaling pathways affects RSC targeting and activity presents a significant future challenge.

Experimental Procedures

Yeast Strains and Plasmids

Strains are listed in Table 1. Gap repair analysis was used to map the temperature-sensitive mutation to the C-terminal 450 bp of *rsc9-1;* this fragment was then sequenced. To generate *RSC9-GFP*, a C-terminal fragment of *RSC9* was amplified by PCR and, along

with a genomic fragment containing the promoter and N terminus of *RSC9,* inserted into pPS934 to create an in-frame *RSC9-GFP* fusion (pPS2292).

FACS Analysis

Cells were grown in YPD at 25°C to log phase and shifted to 37°C for 2, 4, and 6 hr. Cells were fixed overnight in 70% ethanol, sonicated, treated overnight with RNase A, then treated with pepsin, and stained with propidium iodide, as described (Pellman et al., 1995).

Synthetic Lethal Screen

The synthetic lethal screen was based on the colony sectoring assay (Bender and Pringle, 1991). The *rsc9-1* strain was crossed to CH1462 to generate PSY2349 carrying a high copy *RSC9 ADE3 URA3* plasmid (pPS2294). Two synthetic lethal strains were isolated following EMS mutagenesis. Following two backcrosses, the mutations were cloned by complementation with a *URA3 CEN* genomic library (Rose et al., 1987) by screening for sectoring colonies. The ability of subcloned low copy plasmids *STH1 TRP1* and *RSC8 TRP1* (pPS2297 and pPS2300, respectively) to restore 5-FOA resistance to the synthetic lethal strains was confirmed. Linkage was checked by tetrad analysis, and then the *sth1-101* and *rsc8-1* mutations were isolated.

Purification of RSC

RSC purification and protein identifications were performed as described (Cairns et al., 1996). RSC was also partially purified using Rsc9-protein A, where this fusion replaces endogenous Rsc9. Purification was performed at 4°C and monitored by immunoblot analysis. Yeast extract (0.42 g) from PSY2355 was prepared as described (Cairns et al., 1996). Extract was corrected to 450 mM KOAc and passed through DEAE-Sephacel (11 mL, Fast Flow). The flowthrough was dialyzed to 100 mM KOAc in buffer A (50 mM HEPES [pH 7.5], 20% glycerol, 0.5 mM dithiothreitol, 10 mM EDTA, and protease inhibitors) and applied to SP Sepharose (5 ml, Fast Flow). Protein was eluted with a 20 mL linear gradient from 100 mM to 500 mM potassium acetate in buffer B (50 mM HEPES [pH 7.5], 20% glycerol, 2 mM β-mercaptoethanol, and protease inhibitors). Peak fractions were pooled and a portion (1 mg) was bound in batch for 2 hr to IgG-Sepharose (40 μl) in buffer C (10 mM Tris-Cl [pH 8.0], 10% glycerol, and 0.2% Nonidet P-40) containing 200 mM potassium acetate. Bound material was washed four times with 1 ml of buffer C containing 600 mM potassium acetate and eluted with 10% SDS.

Genome-Wide Localization of Rsc9

The genomic copy of *RSC9* was tagged with 18 myc epitopes in strain Z1256, generating PSY2439. The fusion replaces the endogenous copy of *RSC9* and is fully functional. The cells are mating competent and form shmoos in response to α factor. We later discovered that PSY2439 cannot grow on glycerol or acetate and is *rho*$^-$. Importantly, all genome-wide localizations were performed in glucose-containing media. Moreover, our analysis of gene expression profiles in *rho*$^+$ versus *rho*$^-$ cells (Epstein et al., 2001) revealed that the *rho*$^-$ characteristic does not affect the expression of stress-regulated genes in logarithmically growing cells, implying that Rsc9 occupancy is not affected either. For example, at $OD_{600} = 0.5$, profiles of the genes in mitochondrial localization closely match those of the entire set of 6218 genes; only 5%–7% of the genes increases, and 5%–7% decreases more than 2-fold.

The experimental procedure was exactly as described (see Results [Ren et al., 2000]). Cultures were grown in YPD media at 30°C to OD_{600} of 0.6–0.8, and one or none of the following treatments was applied for 30 min: rapamycin (Calbiochem) at 200 nM; hydrogen peroxide (Fisher) at 0.3 mM; and α factor (U.S. Biological) at 50 nM. For the analysis, ORFs were assigned to intergenic regions immediately upstream of their ATG; in cases of diverging ORFs, both were assigned to the same region (Ren et al., 2000). We tested the association between Rsc9-occupied genes and gene annotation in the YPD database (Costanzo et al., 2001) using Fisher's exact test (Keeping, 1995). The reported p values have been corrected for multiple hypothesis testing as follows. We generated 1000 random lists of intergenic sequences, translated them into ORF lists, and subjected each list to the analysis. The 1000 uncorrected p values corresponding to the highest enrichment in each random list were compiled, and the p values from our experimental data were corrected based on this distribution.

Northern Analysis

Cultures were grown as for the genome-wide localization experiments. Cells were treated with rapamycin (200 nM) for the final 30 min of a shift to 37°C. Northern blots were performed with standard procedures (Ausubel et al., 1997). Probes for *PUT1, SDH2, PRB1,* and *ACT1* were labeled with dCTP [α-^{32}P] (NEN Life Sciences, Boston, MA) and a Random Primed DNA Labeling Kit (Roche Molecular Biochemicals). Blots were exposed to a Storage Phosphor screen that was scanned with a Storm 860 (Molecular Dynamics) and analyzed with ImageQuant software. In each sample, *PUT1, SDH2,* and *PRB1* levels were normalized to *ACT1*.

Measurement of rRNA Synthesis

At each time point, 10^7 cells were labeled with 50 μCi of [methyl-^{3}H]methionine for 3 min in a volume of 1 ml (specific activity, >70 μCi/mmole; NEN Life Sciences, Boston, MA). Cells were harvested, washed with 1 ml ice-cold water, and harvested again; the cell pellets were frozen on dry ice. Total RNA was isolated with hot acid phenol (Ausubel et al., 1997).

Acknowledgments

This work was funded by grants from the National Institutes of Health (P.A.S. and B.R.C.), the Howard Hughes Medical Institute (B.R.C.), the European Molecular Biology Organization (I.S.), the National Cancer Institute (P.T.), and by an NIH Training Grant in Tumor Biology (M.D.). The authors are grateful to J. Daley for assistance with FACS and to E. Lei, D. Roberts, and J. Way for helpful discussions.

Received December 20, 2000; revised January 31, 2002.

References

Altschul, S.F., Gish, W., Miller, W., Myers, E.W., and Lipman, D.J. (1990). Basic local alignment search tool. J. Mol. Biol. *215*, 403–410.

Angus-Hill, M.L., Schlichter, A., Roberts, D., Erdjument-Bromage, H., Tempst, P., and Cairns, B.R. (2001). A rsc3/rsc30 zinc cluster dimer reveals novel roles for the chromatin remodeler rsc in gene expression and cell cycle control. Mol. Cell *7*, 741–751.

Ausubel, F.M., Brent, R., Kingston, R.E., Moore, D.D., Seidman, J.G., Smith, J.A., and Struhl, K. (1997). Current Protocols in Molecular Biology (New York: John Wiley & Sons).

Beck, T., and Hall, M.N. (1999). The TOR signalling pathway controls nuclear localization of nutrient- regulated transcription factors. Nature *402*, 689–692.

Bender, A., and Pringle, J.R. (1991). Use of a screen for synthetic lethal and multicopy suppressee mutants to identify two new genes involved in morphogenesis in Saccharomyces cerevisiae. Mol. Cell. Biol. *11*, 1295–1305.

Cairns, B.R., Lorch, Y., Li, Y., Zhang, M., Lacomis, L., Erdjument-Bromage, H., Tempst, P., Du, J., Laurent, B., and Kornberg, R.D. (1996). RSC, an essential, abundant chromatin-remodeling complex. Cell *87*, 1249–1260.

Cairns, B.R., Erdjument-Bromage, H., Tempst, P., Winston, F., and Kornberg, R.D. (1998). Two actin-related proteins are shared functional components of the chromatin-remodeling complexes RSC and SWI/SNF. Mol. Cell *2*, 639–651.

Cairns, B.R., Schlichter, A., Erdjument-Bromage, H., Tempst, P., Kornberg, R.D., and Winston, F. (1999). Two functionally distinct forms of the RSC nucleosome-remodeling complex, containing essential AT hook, BAH, and bromodomains. Mol. Cell *4*, 715–723.

Cao, Y., Cairns, B.R., Kornberg, R.D., and Laurent, B.C. (1997). Sfh1p, a component of a novel chromatin-remodeling complex, is required for cell cycle progression. Mol. Cell. Biol. *17*, 3323–3334.

Cardenas, M.E., Cutler, N.S., Lorenz, M.C., Di Como, C.J., and Heitman, J. (1999). The TOR signaling cascade regulates gene expression in response to nutrients. Genes Dev. *13*, 3271–3279.

Causton, H.C., Ren, B., Koh, S.S., Harbison, C.T., Kanin, E., Jen-

nings, E.G., Lee, T.I., True, H.L., Lander, E.S., and Young, R.A. (2001). Remodeling of yeast genome expression in response to environmental changes. Mol. Biol. Cell *12*, 323–337.

Chan, T.F., Carvalho, J., Riles, L., and Zheng, X.F. (2000). A chemical genomics approach toward understanding the global functions of the target of rapamycin protein (TOR). Proc. Natl. Acad. Sci. USA *97*, 13227–13232.

Cosma, M.P., Tanaka, T., and Nasmyth, K. (1999). Ordered recruitment of transcription and chromatin remodeling factors to a cell cycle- and developmentally regulated promoter. Cell *97*, 299–311.

Costanzo, M.C., Crawford, M.E., Hirschman, J.E., Kranz, J.E., Olsen, P., Robertson, L.S., Skrzypek, M.S., Braun, B.R., Hopkins, K.L., Kondu, P., et al. (2001). YPD, PombePD and WormPD: model organism volumes of the BioKnowledge library, an integrated resource for protein information. Nucleic Acids Res. *29*, 75–79.

Du, J., Nasir, I., Benton, B.K., Kladde, M.P., and Laurent, B.C. (1998). Sth1p, a Saccharomyces cerevisiae Snf2p/Swi2p homolog, is an essential ATPase in RSC and differs from Snf/Swi in its interactions with histones and chromatin-associated proteins. Genetics *150*, 987–1005.

Eisen, M.B., Spellman, P.T., Brown, P.O., and Botstein, D. (1998). Cluster analysis and display of genome-wide expression patterns. Proc. Natl. Acad. Sci. USA *95*, 14863–14868.

Epstein, C.B., Waddle, J.A., Hale, W.T., Dave, V., Thornton, J., Macatee, T.L., Garner, H.R., and Butow, R.A. (2001). Genome-wide responses to mitochondrial dysfunction. Mol. Biol. Cell *12*, 297–308.

Gasch, A.P., Spellman, P.T., Kao, C.M., Carmel-Harel, O., Eisen, M.B., Storz, G., Botstein, D., and Brown, P.O. (2000). Genomic expression programs in the response of yeast cells to environmental changes. Mol. Biol. Cell *11*, 4241–4257.

Gregory, S.L., Kortschak, R.D., Kalionis, B., and Saint, R. (1996). Characterization of the dead ringer gene identifies a novel, highly conserved family of sequence-specific DNA-binding proteins. Mol. Cell. Biol. *16*, 792–799.

Hardwick, J.S., Kuruvilla, F.G., Tong, J.K., Shamji, A.F., and Schreiber, S.L. (1999). Rapamycin-modulated transcription defines the subset of nutrient-sensitive signaling pathways directly controlled by the Tor proteins. Proc. Natl. Acad. Sci. USA *96*, 14866–14870.

Herrscher, R.F., Kaplan, M.H., Lelsz, D.L., Das, C., Scheuermann, R., and Tucker, P.W. (1995). The immunoglobulin heavy-chain matrix-associating regions are bound by Bright: a B cell-specific transactivator that describes a new DNA-binding protein family. Genes Dev. *9*, 3067–3082.

Iwahara, J., and Clubb, R.T. (1999). Solution structure of the DNA binding domain from Dead ringer, a sequence-specific AT-rich interaction domain (ARID). EMBO J. *18*, 6084–6094.

Iyer, V.R., Horak, C.E., Scafe, C.S., Botstein, D., Snyder, M., and Brown, P.O. (2001). Genomic binding sites of the yeast cell-cycle transcription factors SBF and MBF. Nature *409*, 533–538.

Kadonaga, J.T. (1998). Eukaryotic transcription: an interlaced network of transcription factors and chromatin-modifying machines. Cell *92*, 307–313.

Keeping, E.S. (1995). Introduction to Statistical Inference (New York: Dover).

Kingston, R.E., and Narlikar, G.J. (1999). ATP-dependent remodeling and acetylation as regulators of chromatin fluidity. Genes Dev. *13*, 2339–2352.

Laurent, B.C., Yang, X., and Carlson, M. (1992). An essential Saccharomyces cerevisiae gene homologous to SNF2 encodes a helicase-related protein in a new family. Mol. Cell. Biol. *12*, 1893–1902.

Moreira, J.M., and Holmberg, S. (1999). Transcriptional repression of the yeast CHA1 gene requires the chromatin-remodeling complex RSC. EMBO J. *18*, 2836–2844.

Pellman, D., Bagget, M., Tu, Y.H., Fink, G.R., and Tu, H. (1995). Two microtubule-associated proteins required for anaphase spindle movement in Saccharomyces cerevisiae. J. Cell Biol. *130*, 1373–1385.

Powers, T., and Walter, P. (1999). Regulation of ribosome biogenesis by the rapamycin-sensitive TOR- signaling pathway in Saccharomyces cerevisiae. Mol. Biol. Cell *10*, 987–1000.

Ren, B., Robert, F., Wyrick, J.J., Aparicio, O., Jennings, E.G., Simon, I., Zeitlinger, J., Schreiber, J., Hannett, N., Kanin, E., et al. (2000). Genome-wide location and function of DNA binding proteins. Science *290*, 2306–2309.

Roberts, C.J., Nelson, B., Marton, M.J., Stoughton, R., Meyer, M.R., Bennett, H.A., He, Y.D., Dai, H., Walker, W.L., Hughes, T.R., et al. (2000). Signaling and circuitry of multiple MAPK pathways revealed by a matrix of global gene expression profiles. Science *287*, 873–880.

Rohde, J., Heitman, J., and Cardenas, M.E. (2001). The TOR kinases link nutrient sensing to cell growth. J. Biol. Chem. *276*, 9583–9586.

Rose, M., Novick, P., Thomas, J.H., Botstein, D., and Fink, G.R. (1987). A *Saccharomyces cerevisiae* genomic plasmid bank based on centromere-containing shuttle vector. Gene *60*, 237–243.

Schmelzle, T., and Hall, M.N. (2000). TOR, a central controller of cell growth. Cell *103*, 253–262.

Seedorf, M., Damelin, M., Kahana, J., Taura, T., and Silver, P.A. (1999). Interactions between a nuclear transporter and a subset of nuclear pore complex proteins depend on Ran GTPase. Mol. Cell. Biol. *19*, 1547–1557.

Shamji, A.F., Kuruvilla, F.G., and Schreiber, S.L. (2000). Partitioning the transcriptional program induced by rapamycin among the effectors of the Tor proteins. Curr. Biol. *10*, 1574–1581.

Stage-Zimmermann, T., Schmidt, U., and Silver, P.A. (2000). Factors affecting nuclear export of the 60S ribosomal subunit in vivo. Mol. Biol. Cell *11*, 3777–3789.

Treich, I., and Carlson, M. (1997). Interaction of a Swi3 homolog with Sth1 provides evidence for a Swi/Snf- related complex with an essential function in Saccharomyces cerevisiae. Mol. Cell. Biol. *17*, 1768–1775.

Tsuchiya, E., Uno, M., Kiguchi, A., Masuoka, K., Kanemori, Y., Okabe, S., and Mikayawa, T. (1992). The Saccharomyces cerevisiae NPS1 gene, a novel CDC gene which encodes a 160 kDa nuclear protein involved in G2 phase control. EMBO J. *11*, 4017–4026.

Warner, J.R. (1989). Synthesis of ribosomes in Saccharomyces cerevisiae. Microbiol. Rev. *53*, 256–271.

Yukawa, M., Katoh, S., Miyakawa, T., and Tsuchiya, E. (1999). Nps1/Sth1p, a component of an essential chromatin-remodeling complex of Saccharomyces cerevisiae, is required for the maximal expression of early meiotic genes. Genes Cells *4*, 99–110.